EUROPEAN ORGANISATION FOR NUCLEAR RESEARCH

CERN-PPE/93-26
8 February 1993

Evidence for Chain-Like Production of Strange Baryon Pairs in Jets

The OPAL Collaboration

Abstract

The production dynamics of baryon-antibaryon pairs are investigated using hadronic Z^0 decays, recorded with the OPAL detector, which contain at least two identified Λ baryons. The rapidity difference for $\Lambda\overline{\Lambda}$ pairs shows the correlations expected from models with a chain-like production of baryon-antibaryon pairs. If the baryon number of a Λ is compensated by a $\overline{\Lambda}$, the $\overline{\Lambda}$ is found with a probability of 53% in an interval of ± 0.6 around the Λ rapidity. This correlation strength is weaker than predicted by the Herwig Monte Carlo and the Jetset Monte Carlo with a production chain of baryon-antibaryon, and stronger than predicted by the UCLA model. The observed rapidity correlations can be described by the Jetset Monte Carlo with a dominant production chain of baryon-meson-antibaryon, the popcorn mechanism. In addition to the short range correlations, one finds an indication of a correlation of $\Lambda\overline{\Lambda}$ pairs in opposite hemispheres if both the Λ and the $\overline{\Lambda}$ have large rapidities. Such long range correlations are expected if the primary quark flavours are compensated in opposite hemispheres and if these quarks are found in energetic baryons. Rates for simultaneous baryon and strangeness number compensation for $\Lambda\overline{\Lambda}$, $\Xi^-\overline{\Xi}^+$ and $\Xi^-\overline{\Lambda}$ ($\overline{\Xi}^+\Lambda$) are measured and compared with different Monte Carlo models.

(Submitted to Physics Letters B)

The OPAL Collaboration

P.D. Acton[25], G. Alexander[23], J. Allison[16], P.P. Allport[5], K.J. Anderson[9], S. Arcelli[2], A. Astbury[28], D. Axen[29], G. Azuelos[18,a], G.A. Bahan[16], J.T.M. Baines[16], A.H. Ball[17], J. Banks[16], R.J. Barlow[16], S. Barnett[16], J.R. Batley[5], G. Beaudoin[18], A. Beck[23], G.A. Beck[13], J. Becker[10], T. Behnke[27], K.W. Bell[20], G. Bella[23], P. Bentkowski[18], P. Berlich[10], S. Bethke[11], O. Biebel[3], U. Binder[10], I.J. Bloodworth[1], P. Bock[11], B. Boden[3], H.M. Bosch[11], H. Breuker[8], P. Bright-Thomas[25], R.M. Brown[20], A. Buijs[8], H.J. Burckhart[8], C. Burgard[27], P. Capiluppi[2], R.K. Carnegie[6], A.A. Carter[13], J.R. Carter[5], C.Y. Chang[17], D.G. Charlton[8], S.L. Chu[4], P.E.L. Clarke[25], I. Cohen[23], J.C. Clayton[1], W.J. Collins[5], J.E. Conboy[15], M. Cooper[22], M. Coupland[14], M. Cuffiani[2], S. Dado[22], G.M. Dallavalle[2], S. De Jong[13], L.A. del Pozo[5], H. Deng[17], A. Dieckmann[11], M. Dittmar[4], M.S. Dixit[7], E. do Couto e Silva[12], J.E. Duboscq[8], E. Duchovni[26], G. Duckeck[11], I.P. Duerdoth[16], D.J.P. Dumas[6], P.A. Elcombe[5], P.G. Estabrooks[6], E. Etzion[23], H.G. Evans[9], F. Fabbri[2], M. Fierro[2], M. Fincke-Keeler[28], H.M. Fischer[3], D.G. Fong[17], M. Foucher[17], A. Gaidot[21], O. Ganel[26], J.W. Gary[4], J. Gascon[18], R.F. McGowan[16], N.I. Geddes[20], C. Geich-Gimbel[3], S.W. Gensler[9], F.X. Gentit[21], G. Giacomelli[2], R. Giacomelli[2], V. Gibson[5], W.R. Gibson[13], J.D. Gillies[20], J. Goldberg[22], M.J. Goodrick[5], W. Gorn[4], C. Grandi[2], F.C. Grant[5], J. Hagemann[27], G.G. Hanson[12], M. Hansroul[8], C.K. Hargrove[7], P.F. Harrison[13], J. Hart[8], P.M. Hattersley[1], M. Hauschild[8], C.M. Hawkes[8], E. Heflin[4], R.J. Hemingway[6], R.D. Heuer[8], J.C. Hill[5], S.J. Hillier[8], T. Hilse[10], D.A. Hinshaw[18], J.D. Hobbs[8], P.R. Hobson[25], D. Hochman[26], R.J. Homer[1], A.K. Honma[28,a], R.E. Hughes-Jones[16], R. Humbert[10], P. Igo-Kemenes[11], H. Ihssen[11], D.C. Imrie[25], A.C. Janissen[6], A. Jawahery[17], P.W. Jeffreys[20], H. Jeremie[18], M. Jimack[2], M. Jobes[1], R.W.L. Jones[13], P. Jovanovic[1], C. Jui[4], D. Karlen[6], K. Kawagoe[24], T. Kawamoto[24], R.K. Keeler[28], R.G. Kellogg[17], B.W. Kennedy[15], S. Kluth[5], T. Kobayashi[24], D.S. Koetke[8], T.P. Kokott[3], S. Komamiya[24], L. Köpke[8], J.F. Kral[8], R. Kowalewski[6], J. von Krogh[11], J. Kroll[9], M. Kuwano[24], P. Kyberd[13], G.D. Lafferty[16], R. Lahmann[17], F. Lamarche[18], J.G. Layter[4], P. Leblanc[18], A.M. Lee[17], M.H. Lehto[15], D. Lellouch[26], C. Leroy[18], J. Letts[4], S. Levegrün[3], L. Levinson[26], S.L. Lloyd[13], F.K. Loebinger[16], J.M. Lorah[17], B. Lorazo[18], M.J. Losty[7], X.C. Lou[12], J. Ludwig[10], M. Mannelli[8], S. Marcellini[2], G. Maringer[3], C. Markus[3], A.J. Martin[13], J.P. Martin[18], T. Mashimo[24], P. Mättig[3], U. Maur[3], J. McKenna[28], T.J. McMahon[1], J.R. McNutt[25], F. Meijers[8], D. Menszner[11], F.S. Merritt[9], H. Mes[7], A. Michelini[8], R.P. Middleton[20], G. Mikenberg[26], J. Mildenberger[6], D.J. Miller[15], R. Mir[12], W. Mohr[10], C. Moisan[18], A. Montanari[2], T. Mori[24], M. Morii[24], T. Mouthuy[12,b], B. Nellen[3], H.H. Nguyen[9], M. Nozaki[24], S.W. O'Neale[1], F.G. Oakham[7], F. Odorici[2], H.O. Ogren[12], C.J. Oram[28,a], M.J. Oreglia[9], S. Orito[24], J.P. Pansart[21], B. Panzer-Steindel[8], P. Paschievici[26], G.N. Patrick[20], N. Paz-Jaoshvili[23], P. Pfister[10], J.E. Pilcher[9], J. Pinfold[31], D. Pitman[28], D.E. Plane[8], P. Poffenberger[28], B. Poli[2], A. Pouladdej[6], T.W. Pritchard[13], H. Przysiezniak[18], G. Quast[27], M.W. Redmond[9], D.L. Rees[8], G.E. Richards[16], D. Robinson[8], A. Rollnik[3], J.M. Roney[28,c], E. Ros[8], S. Rossberg[10], A.M. Rossi[2], M. Rosvick[28], P. Routenburg[6], K. Runge[10], O. Runolfsson[8], D.R. Rust[12], M. Sasaki[24], C. Sbarra[8], A.D. Schaile[10], O. Schaile[10], W. Schappert[6], P. Scharff-Hansen[8], P. Schenk[4], B. Schmitt[3], H. von der Schmitt[11], S. Schreiber[3], C. Schwick[27], J. Schwiening[3], W.G. Scott[20], M. Settles[12], T.G. Shears[5], B.C. Shen[4], C.H. Shepherd-Themistocleous[7], P. Sherwood[15], R. Shypit[29], A. Simon[3], P. Singh[13], G.P. Siroli[2], A. Skuja[17], A.M. Smith[8], T.J. Smith[28], G.A. Snow[17], R. Sobie[28,c], R.W. Springer[17], M. Sproston[20], K. Stephens[16], J. Steuerer[28], R. Ströhmer[11], D. Strom[30], T. Takeshita[24,d], P. Taras[18], S. Tarem[26], M. Tecchio[9], P. Teixeira-Dias[11], N. Tesch[3], N.J. Thackray[1],

M.A. Thomson[15], E. Torrente-Lujan[22], G. Transtromer[25], N.J. Tresilian[16], T. Tsukamoto[24], M.F. Turner[8], G. Tysarczyk-Niemeyer[11], D. Van den plas[18], R. Van Kooten[27], G.J. VanDalen[4], G. Vasseur[21], C.J. Virtue[7], A. Wagner[27], D.L. Wagner[9], C. Wahl[10], J.P. Walker[1], C.P. Ward[5], D.R. Ward[5], P.M. Watkins[1], A.T. Watson[1], N.K. Watson[8], M. Weber[11], P. Weber[6], P.S. Wells[8], N. Wermes[3], M.A. Whalley[1], G.W. Wilson[4], J.A. Wilson[1], V-H. Winterer[10], T. Wlodek[26], S. Wotton[11], T.R. Wyatt[16], R. Yaari[26], A. Yeaman[13], G. Yekutieli[26], M. Yurko[18], W. Zeuner[8], G.T. Zorn[17].

[1]School of Physics and Space Research, University of Birmingham, Birmingham, B15 2TT, UK
[2]Dipartimento di Fisica dell' Università di Bologna and INFN, Bologna, 40126, Italy
[3]Physikalisches Institut, Universität Bonn, D-5300 Bonn 1, FRG
[4]Department of Physics, University of California, Riverside, CA 92521 USA
[5]Cavendish Laboratory, Cambridge, CB3 0HE, UK
[6]Carleton University, Dept of Physics, Colonel By Drive, Ottawa, Ontario K1S 5B6, Canada
[7]Centre for Research in Particle Physics, Carleton University, Ottawa, Ontario K1S 5B6, Canada
[8]CERN, European Organisation for Particle Physics, 1211 Geneva 23, Switzerland
[9]Enrico Fermi Institute and Department of Physics, University of Chicago, Chicago Illinois 60637, USA
[10]Fakultät für Physik, Albert Ludwigs Universität, D-7800 Freiburg, FRG
[11]Physikalisches Institut, Universität Heidelberg, Heidelberg, FRG
[12]Indiana University, Dept of Physics, Swain Hall West 117, Bloomington, Indiana 47405, USA
[13]Queen Mary and Westfield College, University of London, London, E1 4NS, UK
[14]Birkbeck College, London, WC1E 7HV, UK
[15]University College London, London, WC1E 6BT, UK
[16]Department of Physics, Schuster Laboratory, The University, Manchester, M13 9PL, UK
[17]Department of Physics, University of Maryland, College Park, Maryland 20742, USA
[18]Laboratoire de Physique Nucléaire, Université de Montréal, Montréal, Quebec, H3C 3J7, Canada
[20]Rutherford Appleton Laboratory, Chilton, Didcot, Oxfordshire, OX11 0QX, UK
[21]DAPNIA/SPP, Saclay, F-91191 Gif-sur-Yvette, France
[22]Department of Physics, Technion-Israel Institute of Technology, Haifa 32000, Israel
[23]Department of Physics and Astronomy, Tel Aviv University, Tel Aviv 69978, Israel
[24]International Centre for Elementary Particle Physics and Dept of Physics, University of Tokyo, Tokyo 113, and Kobe University, Kobe 657, Japan
[25]Brunel University, Uxbridge, Middlesex, UB8 3PH UK
[26]Nuclear Physics Department, Weizmann Institute of Science, Rehovot, 76100, Israel
[27]Universität Hamburg/DESY, II Inst für Experimental Physik, 2000 Hamburg 52, Germany
[28]University of Victoria, Dept of Physics, P O Box 3055, Victoria BC V8W 3P6, Canada
[29]University of British Columbia, Dept of Physics, 6224 Agriculture Road, Vancouver BC V6T 1Z1, Canada
[30]University of Oregon, Dept of Physics, Eugene, Oregon 97403, USA
[31]University of Alberta, Dept of Physics, Edmonton AB T6G 2J1, Canada

[a]Also at TRIUMF, Vancouver, Canada V6T 2A3

[b]Now at Centre de Physique des Particules de Marseille, Faculté des Sciences de Luminy, Marseille
[c]And IPP, University of Victoria, Dept of Physics, P O Box 3055, Victoria BC V8W 3P6, Canada
[d]Also at Shinshu University, Matsumoto 390, Japan

1 Introduction

A very general assumption of jet hadronisation is chain-like particle creation with local conservation of quantum numbers, as indicated in figure 1. This assumption is used in jet fragmentation Monte Carlo models like Jetset [1] and Herwig [2], which provide a good description of hadronic events from e^+e^- annihilation. One consequence of a chain-like particle production mechanism is a small rapidity[1] difference between neighbouring particles. Correlations between particle pairs with compensating quantum numbers can be used to test this assumption.

Electric charge correlations in jets have been studied and the results are found to be in agreement with the above assumption [3], but resonance decays and high charged multiplicities make a quantitative interpretation of the results difficult. Measurements of the strangeness or the baryon number compensation mechanism in jets are expected to provide a much cleaner picture of hadron production in jets. However, as indicated in figure 1 two different chains for baryon–antibaryon pairs have been proposed, a chain with either baryon-antibaryon (right half of figure 1) or a chain with baryon–meson–antibaryon (left half of figure 1), the so-called popcorn mechanism [4]. The PETRA and PEP experiments at $\sqrt{s} \approx 30$ GeV could demonstrate that the baryon number is dominantly conserved within the same hemisphere [5], but because of limited statistics, it was not possible to distinguish between various models.

In a previous publication we presented high statistics measurements of inclusive strange baryon production in hadronic Z^0 decays [6]. The cross sections obtained are not all reproduced simultaneously by the baryon production models which are implemented in the Jetset and Herwig Monte Carlos. Furthermore we demonstrated that the popcorn mechanism can not be constrained by the inclusive baryon rates. In this note, we investigate the production dynamics of strange baryon-antibaryon pairs using hadronic events which contain at least two Λ candidates. After a short overview of the experiment and the selection criteria for Λ and Ξ^- particles, the measurements of the rapidity difference of $\Lambda\overline{\Lambda}$ pairs and of the simultaneous compensation of strangeness and baryon number, are described. The results are also compared with predictions of several Monte Carlo models.

2 The OPAL detector

The tracking detectors play a central role in this analysis, and are described briefly below. A detailed description of the entire detector can be found elsewhere [7].

The measurement of the trajectories and momenta of charged particles are performed with a precision vertex chamber, a jet chamber and z-chambers. The cylindrical vertex drift chamber is located between radii of 9 and 24 cm and is subdivided into 36 azimuthal sectors each with 12 anode wires parallel to the beam direction and 36 sectors each with 6 anode wires at an

[1] The rapidity y_i of particle i is defined to be $y_i = 1/2 \times \ln(E_i + p_{i\parallel})/(E_i - p_{i\parallel})$, where E_i is the energy and $p_{i\parallel}$ is the momentum component parallel to the thrust axis.

average stereo angle of 4.1 degrees. In the r-ϕ plane[2], the average space resolution is 50 μm for the hit nearest to the anode wire (first hit) and 90 μm for subsequent hits.

The jet chamber is a large volume drift chamber, 4 m long and 1.85 m in radius, which is divided into 24 azimuthal sectors. Each sector contains a sense-wire plane having 159 axial anode wires. Each of the wires provides three-dimensional coordinate measurements, via drift-time measurement in the r-ϕ plane and charge-division measurement in the z direction. The average space point resolution in the r-ϕ plane is 130 μm. The jet chamber also allows the measurement of the specific energy loss, $\mathrm{d}E/\mathrm{d}x$, of charged particles [8]. A resolution of 3-4% has been obtained allowing particle identification over a large momentum range. In the barrel region ($|\cos\theta|$ less than 0.72), the jet chamber is surrounded by a set of z-chambers covering 94% of the azimuth, each of which has 6 anode wires perpendicular to the beam direction. This provides z coordinate measurements with an accuracy of approximately 300 μm. For larger $|\cos\theta|$ values, the last measured hit on a track can be used to measure θ. The three drift chamber detectors are operated at a gas pressure of 4 bar and are placed inside a solenoidal coil that provides a uniform axial magnetic field of 0.435 T.

Tracks are reconstructed using a method that explicitly incorporates the effect of multiple coulomb scattering in the detector gaseous volumes, in the discrete material between chambers, and in the beam pipe [9]. The momentum resolution in the r-ϕ plane for charged particles in the region $|\cos\theta| < 0.7$ is given by $(\sigma(p_t)/p_t)^2 = 0.02^2 + (0.0018 \cdot p_t)^2$, where p_t is the momentum in the r-ϕ plane in GeV. The impact parameter resolution in the r-ϕ plane, measured using $\mathrm{Z}^0 \to \mu^+\mu^-$ and $\mathrm{Z}^0 \to \mathrm{e}^+\mathrm{e}^-$ decays, is 40 μm for isolated 45 GeV tracks. This resolution degrades to ≈ 65 μm at 10 GeV transverse momentum and to almost 300 μm at 1 GeV due to multiple scattering effects. Angular resolutions are approximately 0.25 mrad in ϕ and 2 mrad in θ for tracks measured in all components of the central detector.

3 Selection of events with Λ and Ξ^- baryons

The data sample, which corresponds to an integrated luminosity of about 20 pb^{-1}, was collected with the OPAL detector at LEP during 1990 and 1991. With the requirement that the three drift chambers are operational, a sample of 485,000 hadronic Z^0 decays has been selected using the criteria described in [10]. For efficiency calculations a sample of approximately 400,000 Jetset hadronic Z^0 decays with full detector simulation is used [11].

To minimize systematics due to edge effects, only events which are well contained in a fiducial volume are used. We demand that the thrust axis points into the barrel region of the detector and require that the polar angle θ_{thrust} fulfils $|\cos\theta_{\mathrm{thrust}}| < 0.8$. In all other aspects, the selection criteria for Λ and Ξ^- candidates are the ones used in [6]. The selection criteria are given below.

[2] The coordinate system is defined such that the z axis follows the electron beam direction, and the x axis is pointing in the direction of the centre of the LEP ring. The radial coordinate, r, is in the $x-y$ plane. The polar and azimuthal angles, θ and ϕ, are defined with respect to the z and x axes, respectively.

3.1 Λ Selection

Λ's are identified by their decays into $p\pi^-$, selecting secondary vertices according to the following criteria:

- all track combinations with opposite charge are examined and the higher momentum track is assigned to be the proton (antiproton) track,
- the momentum of the combination must be greater than 1% of the beam momentum, and the polar angle of the Λ momentum vector is restricted to $|\cos\theta| < 0.9$,
- the impact parameter transverse to the beam direction (d_0) of the pion with respect to the primary vertex[3] must be larger than 3 mm and the d_0 of the proton track must be larger than 0.5 mm,
- background is suppressed by using the information from the $\mathrm{d}E/\mathrm{d}x$ measurement, if available. Because of the cross-over regions which lead to ambiguities in the particle identification [8], momentum dependent cuts are used. If more than 20 hits could be used for the $\mathrm{d}E/\mathrm{d}x$ measurement of a track, the combination is retained only if criterion 1 for the proton and criterion 2 for the pion are fulfilled:

  1. the higher momentum track has to have
     - a $\mathrm{d}E/\mathrm{d}x$ loss of more than 8 keV/cm and the probability[4] for a proton greater than 0.5% if the momentum is less than 1.5 GeV,
     - a $\mathrm{d}E/\mathrm{d}x$ loss of less than 8.5 keV/cm if the momentum is between 1.5 GeV and 2 GeV, where protons and pions both have a specific energy loss of about 7 keV/cm and
     - a probability for a proton of more than 5%, or alternatively the probability for a proton must be larger than the probability for a charged kaon, if the track momentum is above 2 GeV;
  2. for the lower momentum track the probability for a pion must be larger than 0.1%,

- photon conversions are removed if the invariant mass of the track pair, assuming them to be an electron positron pair, is smaller than 40 MeV,
- the selected combinations are required to have at least one track pair intersection within the radial range of 1-130 cm on the side of the primary vertex to which the combined momentum vector points. If two intersections exist, the one closer to the primary vertex is normally used. The second solution is used (a) if both tracks have their first reconstructed hit after the second intersection point or (b) if one track has hits before and the other track has the first hit after the second intersection, and the angle in the plane transverse to the beam direction, Φ, between the direction of flight from the primary vertex to the assumed decay point and the reconstructed Λ momentum, is smaller than for the first intersection,

[3] The primary vertex is fitted for each event using the measured track coordinates in the event.

[4] The difference between the measured and expected $\mathrm{d}E/\mathrm{d}x$ loss for a given particle type, assuming a Gaussian distribution with a known sigma, defines the probability.

- in addition to the track pair intersection cuts described above, a momentum dependent cut on the decay distance is used. It is required that the probability, $e^{-(m_\Lambda/p_t)\cdot(r/c\tau)}$, of the Λ to have not decayed before the calculated radial distance r be less than 95%. This cut excludes Λ's with short decay distances. In addition, for small Λ momenta ($p_t < 1$ GeV), we require that this probability be greater than 2%,
- candidates with hits on both tracks more than 5 cm upstream towards the primary vertex from the track intersection are removed,
- if the reconstructed radial position of the decay point is smaller than 25 cm, it is required that the primary vertex is found between the points of closest approach of the two tracks,
- the angle Φ is required to be smaller than 30 mrad and also smaller than 10 mrad + 20 mrad/$p_t(\Lambda)$, where $p_t(\Lambda)$ is measured in GeV, and
- the angle θ^* between the proton direction in the Λ rest frame and the Λ direction must satisfy $|\cos\theta^*| < 0.98$.

3.2 Ξ^- Selection

Ξ^- are identified by their decays into $\Lambda\pi^-$. Secondary vertices of tracks with the above Λ candidates are selected using the following criteria:

- the d_0 of the additional pion track must be larger than 0.15 mm,
- an intersection of the track and the Λ in the r-ϕ plane must be found within a radial range of 1-50 cm and before the Λ decay point,
- the angle Φ of the $\Lambda\pi$ combination must be smaller than 30 mrad and also smaller than 10 mrad + 20 mrad/$p_t(\Xi)$, and
- if there are more than 20 hits available for the $\mathrm{d}E/\mathrm{d}x$ measurement, the combination is rejected if the probability of the additional track for a pion is smaller than 5% and the probability for an electron or a proton is larger than 5%.

3.3 Number of Events with Strange Baryon Pairs

The Λ signal is defined within a mass region of $\pm$ 10 MeV around its nominal mass of 1115.6 MeV for $x_E(\equiv E_\Lambda/E_{beam})$ smaller than 0.2 and $\pm$ 15 MeV for larger x_E values due to the worsening of the mass resolution. The Ξ^- signal is determined within a mass region of $\pm$ 10 MeV around its nominal mass of 1321.3 MeV, which covers roughly 90% of the signal. The background below the Λ signal is estimated from the sidebands, using the mass intervals between 1090-1100 MeV and 1130-1140 MeV. For the background below the Ξ^- peak, the number of events in the signal region with the wrong charge combination, $\Lambda\pi^+$, is used. With this method a total of 25796 $\pm$ 231 $\Lambda(\overline{\Lambda})$ and 627 $\pm$ 36 $\Xi^-(\overline{\Xi}^+)$ baryons are identified above backgrounds of 13930 and 346, respectively. Further details of the method are given in [6].

Having required that either a $\Lambda(\overline{\Lambda})$ or a $\Xi^-(\overline{\Xi}^+)$ is found in an event, identical criteria are used to look for additional Λ and Ξ^- baryons and the corresponding antibaryons. The $p\pi^-(\overline{p}\pi^+)$ mass spectrum for additional combinations in events with at least one detected $\Lambda(\overline{\Lambda})$ is shown in figure 2a. The mass spectrum for the additional candidates with the same baryon number is shown as a histogram and the one for the candidates with opposite baryon number is shown as points with error bars. Signals for additional Λ's are seen for both combinations, with a large excess of opposite baryon number pairs. The sample with opposite baryon number pair candidates consists of signal pairs where the $\Lambda\overline{\Lambda}$ are produced such that the baryon number is conserved, uncorrelated $\Lambda\overline{\Lambda}$ pairs from events with more than one baryon pair, and pairs in which at least one of the $\Lambda(\overline{\Lambda})$ is combinatorial background. Figure 2b shows the difference of the two distributions in figure 2a. As can be seen from the figures, the combinatorial background outside the Λ mass region is essentially the same for same and opposite baryon number pair candidates. The number of correlated opposite baryon number pairs can be determined from the difference of $\Lambda\overline{\Lambda}$ and $\Lambda\Lambda(\overline{\Lambda}\,\overline{\Lambda})$ pairs. One finds an excess of 990 $\pm$ 54 pairs with opposite baryon number in the Λ signal region.

The number of pair candidates with the same baryon number has been determined to be 485 $\pm$ 60 above a background of 460, using a fit with a Gaussian distribution for the signal and a background function as described in [6]. To determine the number of same baryon number pairs one must take into account background in the tagging $\Lambda(\overline{\Lambda})$ sample, which has a signal to background ratio of 1.85:1. Under the assumption that no correlated production of same baryon number pairs occurs, 35% of the pair candidates will have a background combination as the tag. Taking this background into account a total of 315 $\pm$ 60 $\Lambda\Lambda$ and $\overline{\Lambda}\,\overline{\Lambda}$ pairs above a total background of 630 is obtained. The number of pairs with a background tag and an additional Λ has also been determined using combinations in the sidebands around the Λ signal mass interval to be 192 $\pm$ 30. Subtracting this number from the 485 $\pm$ 60 candidate pairs one obtains 293 $\pm$ 67 in good agreement with the above number.

As a cross check, the number of opposite baryon number pairs can also be determined using a fit. With this method, the sample of $\Lambda\overline{\Lambda}$ pair candidates is determined to be 1335 $\pm$ 100 above a background of 600. This sample contains some contribution from uncorrelated pairs and combinations where the tag is background. This contribution can be estimated from the same baryon number pair candidates, where we found 485 $\pm$ 60 such pairs. After subtraction of this background one obtains 850 $\pm$ 117 excess opposite baryon number pairs, about one standard deviation lower than the number of 990 $\pm$ 54 pairs estimated from the subtraction method. Some of this difference is expected since the non-Gaussian tails will give rise to an overestimation of the background in the fitting method.

For events with an identified $\Xi^-(\overline{\Xi}^+)$, the resulting invariant mass spectra for additional $\overline{p}\pi^+(p\pi^-)$ combinations are shown in figure 2c. An excess of 61 $\pm$ 12 $\Xi^-\overline{\Lambda}(\overline{\Xi}^+\Lambda)$ is found. The resulting mass spectrum for additional $\overline{\Lambda}\pi^+(\Lambda\pi^-)$ combinations is shown in figure 2d. Two pair candidates of the type $\Xi^-\overline{\Xi}^+$ and no pairs with the same baryon number are found in the signal region of $\pm$ 10 MeV around the nominal Ξ^- mass. From the events in sidebands we estimate a background of roughly 1 $\pm$ 1 event in the signal region.

The invariant mass spectra of $\Lambda\overline{\Lambda}$ pair candidates (including background) has been determined over the entire mass range and no resonance-like enhancement has been seen. The mass spectra are well described by the Jetset events with full detector simulation. The mass spectra

type of pair	signal	background	N_{pairs}/event
$\Lambda\overline{\Lambda}$	990 $\pm$ 54	945	0.0621 $\pm$ 0.0034 (stat.) $\pm$ 0.0084 (syst.)
$\Xi^-\overline{\Lambda}(\overline{\Xi}^+\Lambda)$	61 $\pm$ 12	45	0.0096 $\pm$ 0.0019 (stat.) $\pm$ 0.0013 (syst.)
$\Xi^-\overline{\Xi}^+$	1 $\pm$ 1.7	1	0.00038 $\pm$ 0.00067(stat.) $\pm$ 0.00007 (syst.)
$\Lambda\Lambda(\overline{\Lambda}\,\overline{\Lambda})$	315 $\pm$ 60	630	0.0205 $\pm$ 0.0039 (stat.) $\pm$ 0.0028 (syst.)

Table 1: Observed number of opposite and same baryon number pair candidates for different types of combinations, as well as backgrounds and efficiency corrected pair rates per hadronic event. Note that for the pairs with opposite baryon number, the number of correlated pairs is given, i.e. the difference between the total opposite and same baryon number pairs.

for pairs with opposite and same baryon number are shown in figures 3a and 3b for the mass region between 2.2 and 3 GeV.

Using Monte Carlo events which contain an identified $\Lambda(\overline{\Lambda})$, the efficiency of finding a second $\Lambda(\overline{\Lambda})$ in an event was studied and was found to be independent of the presence of the first $\Lambda(\overline{\Lambda})$. Furthermore, the momentum dependent efficiency to find a second Λ was found to be the same as the efficiency to find a single Λ. The detection efficiency, defined for $\Lambda(\overline{\Lambda})$ produced in accepted hadronic events (the thrust axis has to point into the barrel region of the detector) and the decay $\Lambda \rightarrow p\pi^-$ rises steeply from 7.7% for momenta of about 0.5 GeV to a maximum of about 40% for momenta between 2.5 GeV and 5 GeV and decreases slowly to about 10% at 25 GeV. Furthermore, we find that the momentum dependent efficiency to find a $\Lambda(\overline{\Lambda})$ can be used to correct the rapidity distribution. This is demonstrated in figures 4a and 4b. Figure 4a shows the generated Monte Carlo rapidity distribution of $\Lambda(\overline{\Lambda})$ and the rapidity distribution of reconstructed $\Lambda(\overline{\Lambda})$ corrected for the momentum dependent efficiency. Good agreement between the two distributions is obtained. Figure 4b shows the rapidity distributions of generated and efficiency corrected $\overline{\Lambda}$ particles in events containing a detected Λ. Again the two distributions are in good agreement. After correcting for efficiency the pair production rates per hadronic event are given in table 1 together with the observed number of pair candidates for the various channels. To estimate the systematic error of the pair rates we use the systematic errors of the inclusive cross section measurements of Λ and Ξ^- baryons, which were estimated in [6] to be 8% and 9%, respectively. To calculate the pair rate the background error enters once and the efficiency errors enter twice. The total systematic error is therefore 13.5% for the pair rates involving $\Lambda(\overline{\Lambda})$ and 18% for the $\Xi^-\overline{\Xi}^+$ rate.

4 Study of Rapidity and Strangeness Correlations

4.1 Rapidity Correlations

The identified baryon pairs are used to measure the correlation strength in rapidity space. To measure the strength of the rapidity correlation for a true $\Lambda\overline{\Lambda}$ pair, the combinatorial background and the background from events which contain more than one baryon-antibaryon pair have to be corrected for. From a study of Monte Carlo events with two or more baryon

pairs one finds that the rapidity difference Δy of the unassociated pairs with opposite baryon number and the combinatorial background are reproduced by the pairs with the same baryon number. We conclude that both of these backgrounds are simultaneously described by the pair candidates with the same baryon number. Therefore, the same baryon number pair distributions are subtracted in the following analysis from the distributions of pairs with opposite baryon number. The efficiency to find a $\Lambda(\overline{\Lambda})$ has been found to be unaffected by the presence of another $\Lambda(\overline{\Lambda})$ in the same event. In the following studies the measured distributions are corrected for detection efficiency. This allows a simple and direct comparison of the data with Monte Carlo models.

In the case of pairs with opposite baryon number, the Λ is regarded as the tagging particle and its rapidity is defined to be greater than zero. In the case of a pair with the same baryon number the tagging particle is chosen randomly. For this measurement the data are divided into five rapidity subsamples according to the rapidity of the tagging particle. The rapidities of the two baryons are then shifted such that the rapidity of the tagging particle is centred in the appropriate rapidity interval, while the rapidity difference remains unchanged. The rapidity distribution of the $\overline{\Lambda}$ corrected for background and efficiency is shown in figure 5a for the five rapidity intervals of the tagging Λ for the data and the Jetset Monte Carlo with the production chain baryon-antibaryon[5]. The corresponding distributions for pair candidates, including background, with the same baryon number are shown in figure 5b. Strong rapidity correlations are clearly seen over the entire rapidity range for the pairs with opposite baryon number whereas the same baryon number pairs show an essentially flat rapidity distribution for the second Λ, as expected from uncorrelated production. The observed rapidity correlations show evidence for a chain-like production of baryon-antibaryon pairs and are qualitatively reproduced by the Jetset and Herwig Monte Carlos.

To obtain a more quantitative statement about the rapidity correlation strength, the rapidity difference of all $\Lambda\overline{\Lambda}$ pairs is used. The normalized distribution of the rapidity difference $1/N_{pairs}\ dn/d\Delta y$, again corrected for efficiency and the uncorrelated background as determined from the same baryon number pairs, is shown in figures 6a and 6b. The distributions become asymmetric for large rapidity differences because of the limited phase space to find both baryons in the same hemisphere. If the baryon number of a Λ is compensated by a $\overline{\Lambda}$, the $\overline{\Lambda}$ is found with a probability of 53% in an interval of ± 0.6 around the Λ rapidity. The distributions obtained from the Herwig Monte Carlo and the Jetset Monte Carlo with a popcorn parameter of zero are also shown in figure 6a. Both models predict smaller rapidity differences than found in the data. A variation of different parameters within the Herwig Monte Carlo [12] did not result in a significant change of the rapidity difference for $\Lambda\overline{\Lambda}$ pairs. The prediction from the UCLA model [13], with a different ansatz to describe the fragmentation and the popcorn mechanism (on average about 1.7 mesons are produced in between the baryon antibaryon pair) is also shown in figure 6a. It predicts weaker rapidity correlations than the data.

The rapidity difference distribution within Jetset is sensitive only to the choice of the popcorn parameter, which enables the production of baryon-meson-antibaryon configurations [4]. Within this model one can thus compare the observed rapidity correlation strength with different choices for the popcorn parameter. Figure 6b shows the rapidity difference in the data and the Jetset Monte Carlo for 0%, 80%, and 95% probability of the popcorn chain baryon-meson-

[5] A popcorn parameter of zero is used.

antibaryon. The distribution for the default value of 50% popcorn probability has a peak value roughly at the average between the ones for the 0% and 80% distributions. Agreement with the data is obtained for large parameter values, indicating a probability of more than 80% for the production chain baryon-meson-antibaryon.

Long range correlations in opposite hemispheres are expected in addition to the short range correlations for $\Lambda\overline{\Lambda}$ pairs, if two baryon-antibaryon pairs are produced independently and if the Λ and $\overline{\Lambda}$ contain the primary quarks or are the decay products of hadrons which contained the primary quark. For the rapidity interval of the tagging Λ between 1.5 and 3.5 a total of 827 opposite and 374 same baryon number pairs are found. Out of these pairs, we observe 118 $\Lambda\overline{\Lambda}$ candidates in the opposite hemisphere where the $\overline{\Lambda}$ has a rapidity less than –1.5. This is slightly larger than the corresponding number of 82 same baryon number pairs in the same rapidity range. The observed excess of 36 $\pm$ 14 $\Lambda(\overline{\Lambda})$ pairs can be compared with an expectation of 21 $\pm$ 13 from the Monte Carlo with full detector simulation. This excess represents 7.9 $\pm$ 3.1 % of all correlated pairs found for the tagging rapidity interval between 1.5 and 3.5, in agreement with the prediction from Jetset at the generator level, where one expects that 5.5 $\pm$ 0.5 % of all pairs with such large rapidities are found in opposite hemispheres. For a detailed study of such long range correlations more statistics is needed.

4.2 Simultaneous Baryon and Strangeness Compensation

In this section we investigate strange baryon pairs to measure how often strangeness and baryon number are compensated by a strange antibaryon. In chain-like models of baryon production, the strangeness and baryon number of a Λ can be compensated by a $\overline{\Lambda}$ or a $\overline{\Sigma}$, or non-simultaneously by an $\overline{\mathrm{p}}$ or $\overline{\mathrm{n}}$ followed in the chain by a kaon. It is thus interesting to measure how often strangeness and baryon number are compensated together.

To measure this compensation quantitatively, we define the probability P which relates the acceptance corrected inclusive baryon rates $N_{\mathrm{B}(\overline{\mathrm{B}})}$ and the baryon pair rates N_{pairs} per hadronic event (given in table 1). In the cases in which we tag on both types of baryon in the pair, such as with $\Lambda\overline{\Lambda}$ pairs, the probability is

$$P = 2 \times \frac{N_{\mathrm{pairs}}}{N_{\mathrm{B}(\overline{\mathrm{B}})}} \; .$$

The factor of two is necessary since each pair is counted only once but has two baryons of the tagging type. In the case of $\Xi^-\overline{\Lambda}(\overline{\Xi}^+\Lambda)$ pairs, where there is no ambiguity between the tagging and tagged baryon, one drops the factor of two.

In table 2, the measured probabilities are given together with our recent results on inclusive strange meson and baryon production [6], [14]. Since the systematic errors from the inclusive measurements enter only once, we use systematic errors of 8% for the probabilities involving $\Lambda(\overline{\Lambda})$ and 9% for the $\Xi^-\overline{\Xi}^+$ probability.

In our previous publication on strange baryons [6] we showed that the popcorn parameter, which regulates the probability to produce the chain baryon-meson-antibaryon, is not constrained by the inclusive rates. It was also shown that, without additional experimental

results, it is not possible to obtain strong constraints on the various diquark parameters, which regulate the different octet and decuplet baryon yields. It was also found that the measured $\Lambda(\overline{\Lambda})$ momentum spectrum was softer than that predicted and that the different decuplet baryon rates can not be described simultaneously by either of the Monte Carlo models studied.

Table 2 compares the baryon pair production results with the predictions from different models. For this comparison we follow our previous scheme and tune the Monte Carlo parameters so that the measured K^0, $K^*(892)^0$, $\phi(1020)$ and Λ yields and, if possible, the Ξ^- and one of the decuplet baryon yields are described. Because a larger fraction of Λ's originate from $\Sigma(1385)^{\pm}$ decays than from $\Xi(1530)^0$ decays, the spin 1 suppression parameter inside Jetset is tuned to describe the measured $\Sigma(1385)^{\pm}$ yields. The parameters used to obtain the Monte Carlo results are given in [12,13,15].

		probability				
tagging baryon	tagged baryon	OPAL data	Jetset no popcorn	Jetset 95% popcorn	UCLA [13]	Herwig 55 tuned [12]
Λ	$\overline{\Lambda}$	0.354± 0.034	0.291	0.235	0.398	0.374
$\Xi^-(\overline{\Xi}^+)$	$\overline{\Lambda}(\Lambda)$	0.463± 0.099	0.589	0.412	0.580	0.860
Ξ^-	$\overline{\Xi}^+$	0.037 ± 0.065	0.172	0.071	0.082	0.225
$\Lambda(\overline{\Lambda})$	$\Lambda(\overline{\Lambda})$	0.117± 0.024	0.151	0.129	0.117	0.144
particle		N/event				
Λ		0.351± 0.019	0.365	0.336	0.330	0.348
Ξ^-		0.0206± 0.0021	0.0210	0.0205	0.0229	0.0212
$\Sigma(1385)^{\pm}$		0.0380± 0.0062	0.0375	0.0364	0.0756	0.135
$\Xi(1530)^0$		0.0063± 0.0014	0.0023	0.0021	0.0088	0.0073
Ω^-		0.0050± 0.0015	0.0002	0.0002	0.0010	0.0018
K^0		2.10 ± 0.14	2.06	2.04	2.02	2.17
$K^*(892)^0$		0.76 ± 0.09	0.63	0.62	0.73	0.83
$\phi(1020)$		0.086 ± 0.018	0.103	0.101	0.125	0.127

Table 2: Probabilities to find an additional Λ or Ξ^- in events which already contain a Λ or a Ξ^-. The measured inclusive particle (and antiparticle) yields are also given. The errors are the combined statistical and systematic errors.

Within the Jetset Monte Carlo, the inclusive pair production yields of $\Lambda\overline{\Lambda}$, $\Xi^-\overline{\Lambda}$, and $\Xi^-\overline{\Xi}^+$ are determined primarily by the strange diquark suppression factor and the popcorn parameter. The measured probability for $\Lambda\overline{\Lambda}$ pairs is described by Jetset without the popcorn mechanism, while the probabilities for pairs involving Ξ^- baryons are too high. Once the popcorn mechanism is tuned to describe the rapidity difference, the corresponding probabilities for $\Lambda\overline{\Lambda}$ pairs are too small and the ones for Ξ^- pairs are reasonably well described. The UCLA model describes several measurements quite well. However this model overestimates the $\Sigma(1385)^{\pm}$ rates and predicts rapidity correlations weaker than those that we observe. With a tuned version of the Herwig 55 program a reasonable description of the inclusive single strange baryon rates (Λ, Ξ^-, and $\Xi(1530)^0$) and of the probability for $\Lambda\overline{\Lambda}$ pairs is obtained. However, the predicted

$\Sigma(1385)^{\pm}$ yields are much too large, the rapidity correlations of $\Lambda\overline{\Lambda}$ pairs are too strong, and the probabilities to produce pairs which include Ξ^- baryons are overestimated.

5 Summary

Evidence for a correlated production of $\Lambda\overline{\Lambda}$ pairs in rapidity space is shown. Qualitatively this correlation is reproduced in chain-like baryon production models as implemented in the Herwig and Jetset Monte Carlo models. However, the production chain of only baryon-antibaryon pairs predicts stronger rapidity correlations than are observed. In contrast, if 80% or more baryon pairs are produced in the sequence baryon-meson-antibaryon, the observed rapidity difference between $\Lambda\overline{\Lambda}$ pairs is described. The UCLA model, with a larger probability for popcorn mesons, predicts rapidity correlations weaker than those observed. In addition to the short range correlations, an indication of a long range compensation of the strangeness is seen if the Λ and the $\overline{\Lambda}$ are found in opposite hemispheres and at high rapidity values. Such long range correlations are expected if the primary quark flavours are compensated in opposite hemispheres and if these quarks are found in energetic baryons.

The measurement of simultaneous strangeness and baryon number compensation shows that events which contain a $\Lambda(\overline{\Lambda})$ are compensated 35.4 ± 3.4 % of the time by a $\overline{\Lambda}(\Lambda)$ and that events which contain a Ξ^- are compensated 46.3 ± 9.9 % of the time by a $\overline{\Lambda}$ and in 3.7 ± 6.5% of the cases by a $\overline{\Xi}^+$.

So far no parametrisation of the various models has been found which gives a satisfactory description of both the observed rapidity difference of $\Lambda\overline{\Lambda}$ pairs and the measured simultaneous baryon and strangeness number compensation. However, since the rapidity difference distribution is presumably more sensitive to the underlying fragmentation dynamics and perhaps even independent of the baryon species that is produced, the observed rapidity correlations indicate that the popcorn chain, baryon–meson–antibaryon, is likely to occur with a high probability.

Acknowledgements

We are grateful to T. Sjöstrand, B. Webber and. C. D. Buchanan for various interesting discussions about this analysis.
It is a pleasure to thank the SL Division for the efficient operation of the LEP accelerator, the precise information on the absolute energy, and their continuing close cooperation with our experimental group. In addition to the support staff at our own institutions we are pleased to acknowledge the
Department of Energy, USA,
National Science Foundation, USA,
Texas National Research Laboratory Commission, USA,
Science and Engineering Research Council, UK,
Natural Sciences and Engineering Research Council, Canada,
Fussefeld Foundation,
Israeli Ministry of Energy,
Israeli Ministry of Science,
Minerva Gesellschaft,

Japanese Ministry of Education, Science and Culture (the Monbusho) and a grant under the Monbusho International Science Research Program,
German Israeli Bi-national Science Foundation (GIF),
Direction des Sciences de la Matière du Commissariat à l'Energie Atomique, France,
Bundesministerium für Forschung und Technologie, FRG,
National Research Council of Canada, Canada,
A.P. Sloan Foundation and Junta Nacional de Investigação Científica e Tecnológica, Portugal.

References

[1] B. Andersson *et al.*, Phys. Rep. **97** (1983) 31;
T. Sjöstrand, Comp. Phys. Comm. **39** (1986) 347 and CERN-TH.6488/92;
T. Sjöstrand and M. Bengtsson, Comp. Phys. Comm. **43** (1987) 367.

[2] G. Marchesini *et al.*, Cambridge preprint Cavendish-HEP-91/26 and DESY 91-048.

[3] See for example: P. Mättig, Phys. Rep. **177** (1989) 141.

[4] B. Andersson, G. Gustafson and T. Sjöstrand, Physica Scripta **32** (1985) 574.
A popcorn model has been implemented in Jetset, where the frequency for the process baryon-meson-antibaryon is regulated by the parameter PARJ(5), such that the probability is given by PARJ(5)/(0.5 + PARJ(5)).

[5] JADE Collab., W. Bartel *et al.*, Phys. Lett. **B104** (1981) 325;
TASSO Collab., M. Althoff *et al.*, Z. Phys. **C17** (1983) 5; **C27** (1985) 27 and Phys. Lett. **B139** (1984) 126;
TPC Collab., H. Aihara *et al.*, Phys. Rev. Lett. **53** (1984) 2199; **54** (1985) 274 and **55** (1985) 1047;
MARK2 Collab., C. de la Vaissiere *et al.*, Phys. Rev. Lett. **54** (1985) 2071;
HRS Collab., M. Derrick *et al.*, Phys. Rev. **D35** (1987) 2639.

[6] OPAL Collab., P. D. Acton *et al.*, Phys. Lett. **B291** (1992) 503.

[7] OPAL Collab., M. Ahmet *et al.*, Nucl. Instrum. and Meth. **A305** (1991) 275.

[8] M. Hauschild *et al.*, Nucl. Instrum. and Meth. **A314** (1992) 74.

[9] P. Billoir, Nucl. Instrum. and Meth. **225** (1984) 352.

[10] OPAL Collaboration, G. Alexander *et al.*, Z. Phys. **C52** (1991) 175.

[11] J. Allison *et al.*, Nucl. Instrum. and Meth. **A317** (1992) 47.

[12] For the tuned Herwig 55 we use: CLMAX=2.52, CLPOW=1.12, QDIQK=2.1 and PDIQK=5.0 and increase the s-quark mass from 0.5 to 0.6 GeV.

[13] S. B. Chun and C.D. Buchanan, UCLA-HEP-92-008. The quoted results were obtained directly from the authors. They have used values of η=2.5 a= 1.9 and b=1.1, for more details we refer to the above reference.

[14] OPAL Collab., G. Alexander *et al.*, Phys. Lett. **B264** (1991) 467; and P.D. Acton *et al.* CERN-PPE/92-116.

[15] The results for Jetset are obtained with the following non-default parameters for meson production of PARJ(2)=0.26, PARJ(11)=0.45 and PARJ(12)=0.35. These values have been changed with respect to those in our previous publication [6] in order to obtain a better description of the inclusive vector meson $K^*(892)^0$ and $\phi(1020)$ yields [14].
The non-default baryon production parameters for 0% popcorn probability (PARJ(5)=0) are PARJ(3)=0.26 and PARJ(4)= 0.04; for 95% popcorn probability (PARJ(5)=9.5) we use PARJ(3)=0.32 and PARJ(4)= 0.0025.

Figure Captions

Figure 1: Schematic diagrams which show the chain-like quark-diquark–diquark–quark production of baryon-antibaryon pairs (right side) and an example of the popcorn mechanism with a chain antibaryon-meson-baryon (left side).

Figure 2a: Invariant mass of $p\pi^-$ for additional $\Lambda(\overline{\Lambda})$ candidates in events with one identified $\Lambda(\overline{\Lambda})$. The mass distribution for events with opposite baryon number is shown as points with error bars and the one with the same baryon number as histogram.

Figure 2b: Difference of the two histograms in figure 2a.

Figure 2c: Invariant mass of $p\pi^-$ for additional $\Lambda(\overline{\Lambda})$ candidates in events with one identified $\Xi^-(\overline{\Xi}^+)$. The mass distribution for events with opposite baryon number is shown as points with error bars and the one with the same baryon number as histogram.

Figure 2d: Invariant mass distribution of $\overline{\Lambda}\pi^+$ for events with one identified Ξ^-, the pair with the same baryon number shown as histogram.

Figure 3: Invariant mass of all pair candidates, including background, for (a) $\Lambda\overline{\Lambda}$ pairs and (b) $\Lambda\Lambda$ and $\overline{\Lambda}\,\overline{\Lambda}$ pairs (b). The corresponding distributions from the Monte Carlo with full detector simulation, normalized to the number of pairs, are also shown.

Figure 4a: Generated (histogram) and reconstructed (points with error bars) full Monte Carlo $\Lambda(\overline{\Lambda})$ rapidity distribution. The reconstructed rapidity distribution is corrected for the momentum dependent efficiency.

Figure 4b: Same distributions as in figure 4a, but for $\overline{\Lambda}$'s in Monte Carlo events which contain a detected Λ.

Figure 5a: Rapidity distribution of $\overline{\Lambda}$ for various tagging intervals of Λ's (shown as solid boxes). The uncorrelated background from pair combinations with the same baryon number is subtracted. Negative values, suppressed in the figure, are of negligible amount.

Figure 5b: Rapidity distribution of the second Λ, including background, for various tagging intervals of the first Λ's (shown as solid boxes) for combinations with the same baryon number.

Figure 6a: Rapidity difference, corrected for efficiency, for all $\Lambda\overline{\Lambda}$ pairs (same baryon number pairs are subtracted). The distributions expected from the Herwig, Jetset without popcorn splitting, and UCLA Monte Carlo models are also shown.

Figure 6b: Rapidity difference, corrected for efficiency, for all $\Lambda\overline{\Lambda}$ pairs (same baryon number pairs are subtracted). The distributions expected from the Jetset Monte Carlo with a popcorn production of 0%, 80% and 95% are also shown.

Figure 1

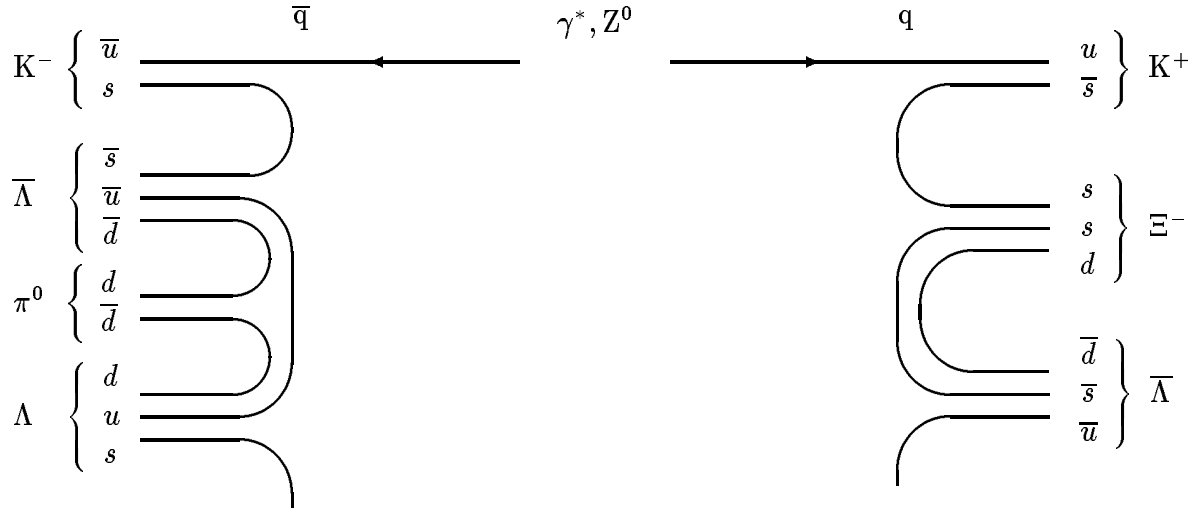
$\overline{\mathrm{q}}$
γ^*, Z^0
q
K^-
$\overline{u}$
s
$\overline{\Lambda}$
$\overline{s}$
$\overline{u}$
$\overline{d}$
π^0
d
$\overline{d}$
Λ
d
u
s
u
$\overline{s}$
K^+
s
s
d
Ξ^-
$\overline{d}$
$\overline{s}$
$\overline{u}$
$\overline{\Lambda}$

Figures 2a, 2b

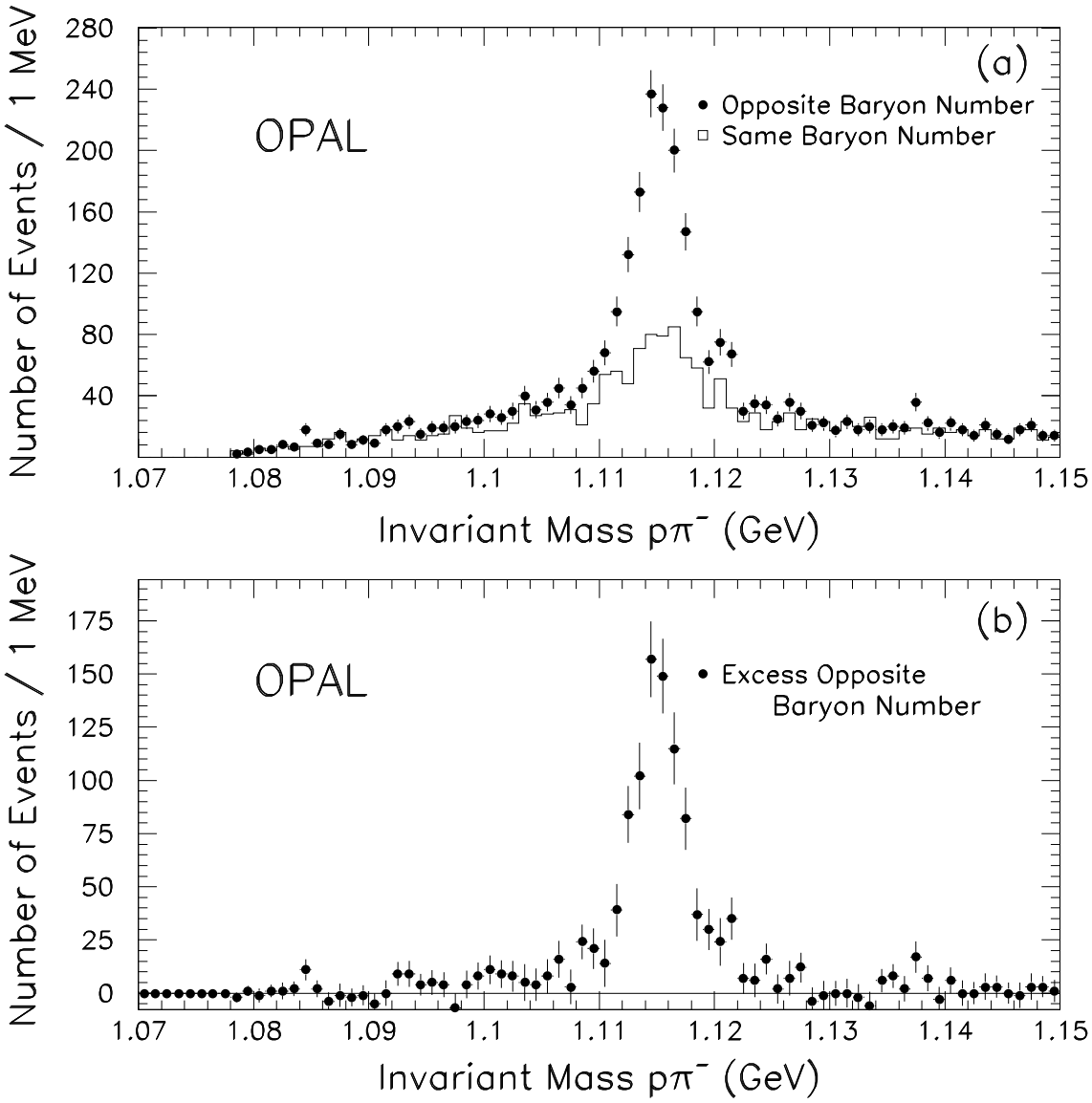

Figures 2c, 2d

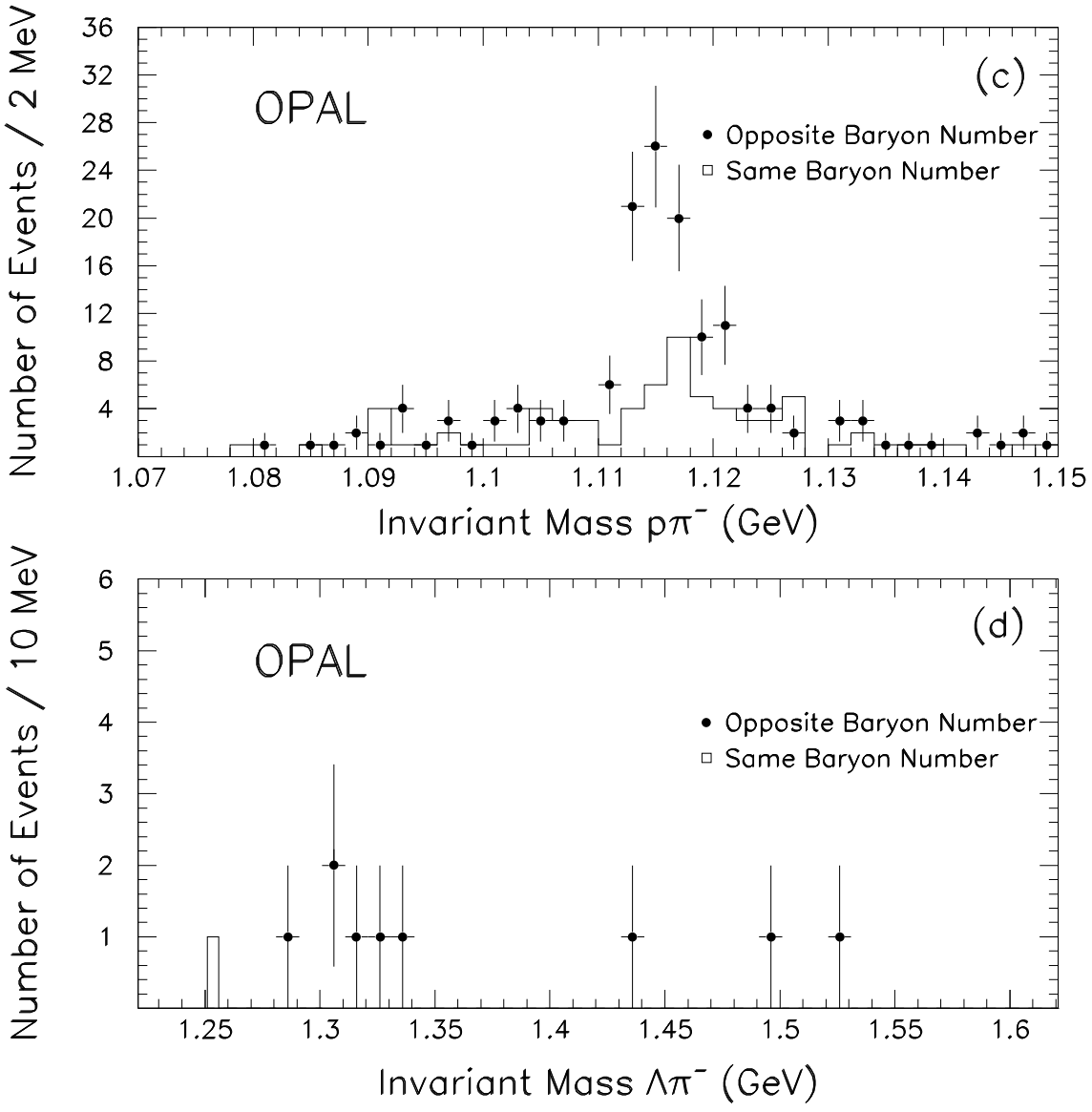

Figures 3a, 3b

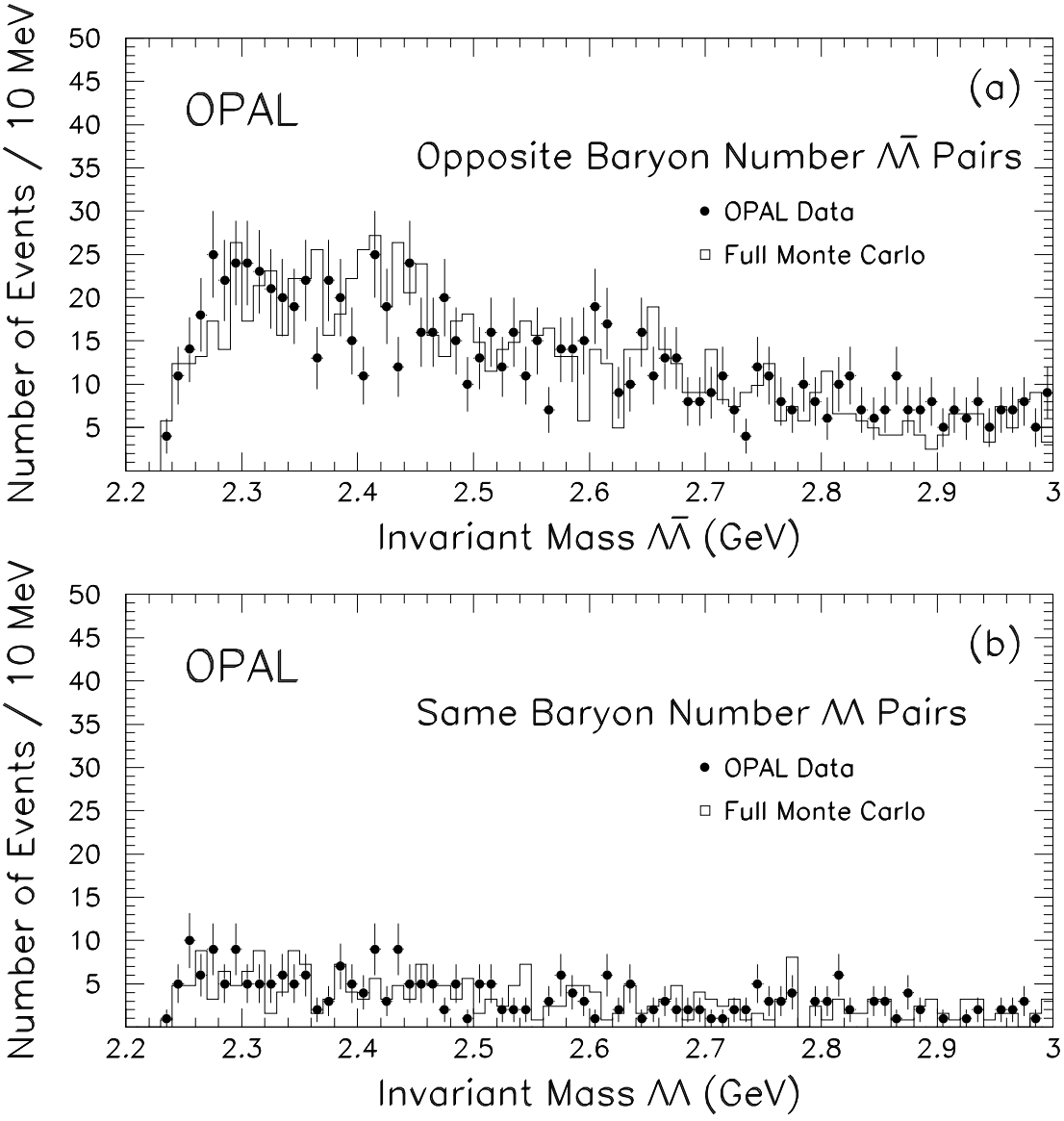

Figures 4a, 4b

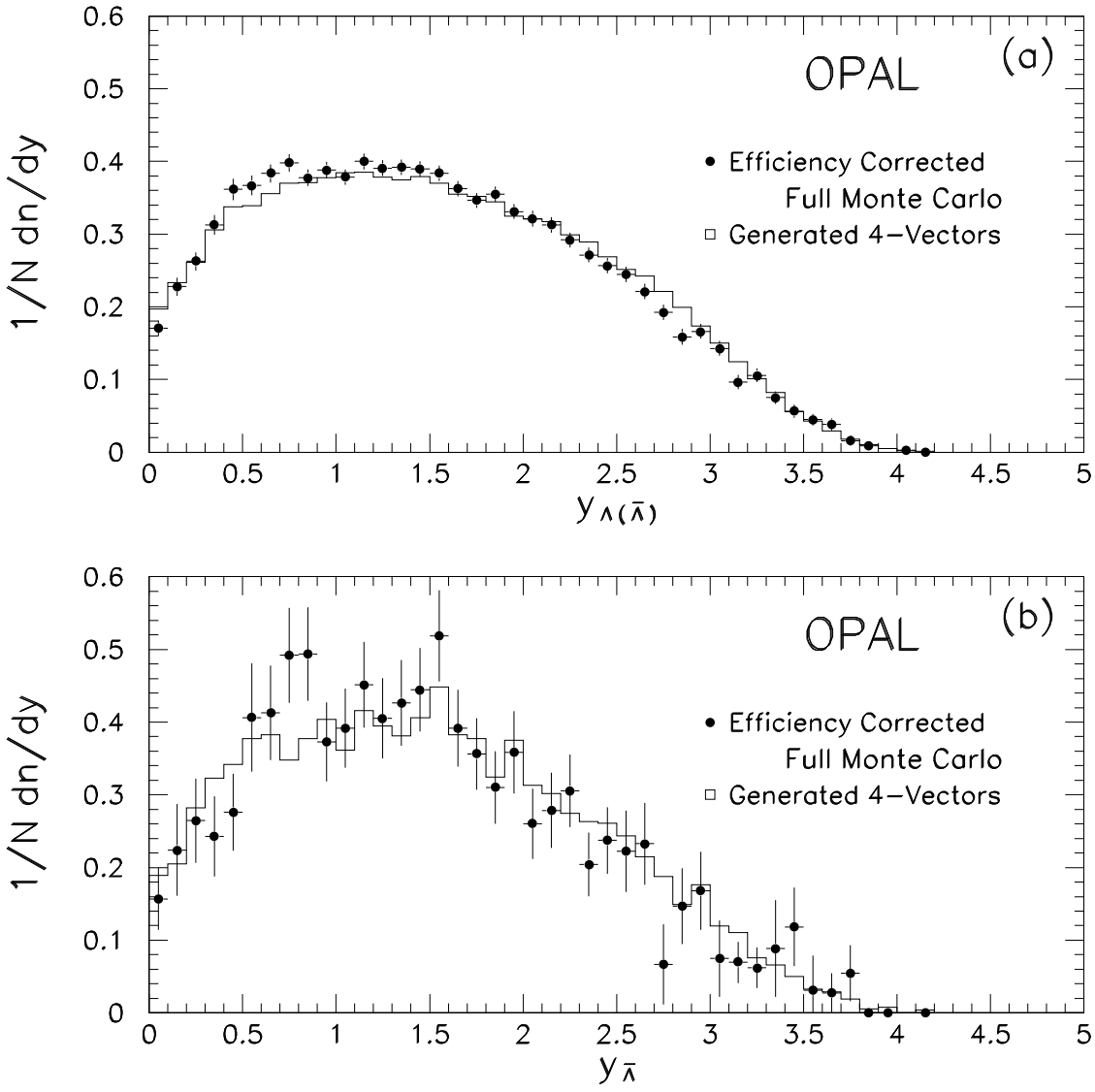

Figure 5a

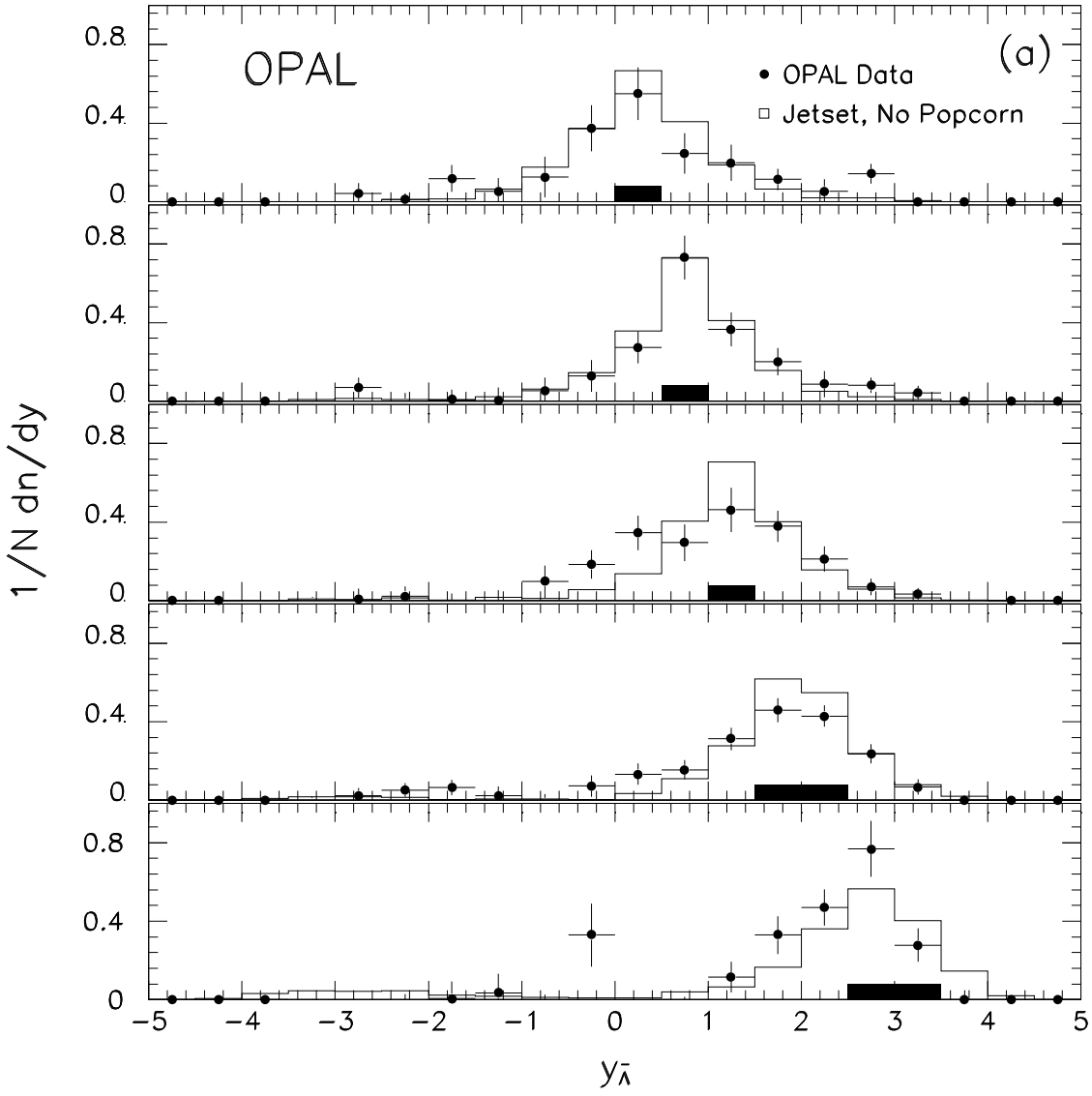
OPAL
(a)
• OPAL Data
□ Jetset, No Popcorn
1/N dn/dy
0.8
0.4
0
−5
−4
−3
−2
−1
0
1
2
3
4
5
$y_{\bar{\Lambda}}$

Figure 5b

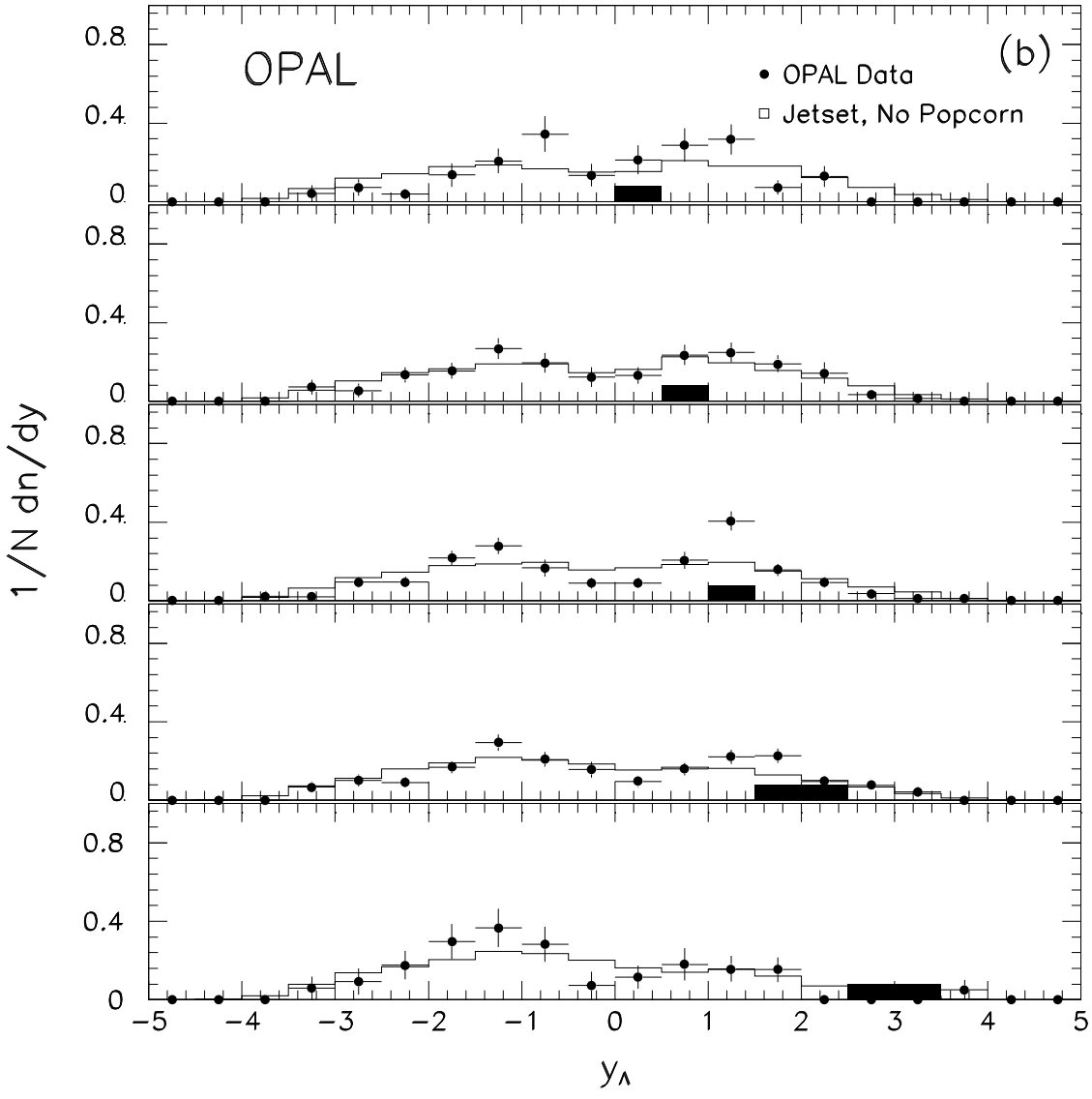
OPAL
(b)
• OPAL Data
□ Jetset, No Popcorn
1/N dn/dy
0.8
0.4
0
−5
−4
−3
−2
−1
0
1
2
3
4
5
y_Λ

Figure 6a

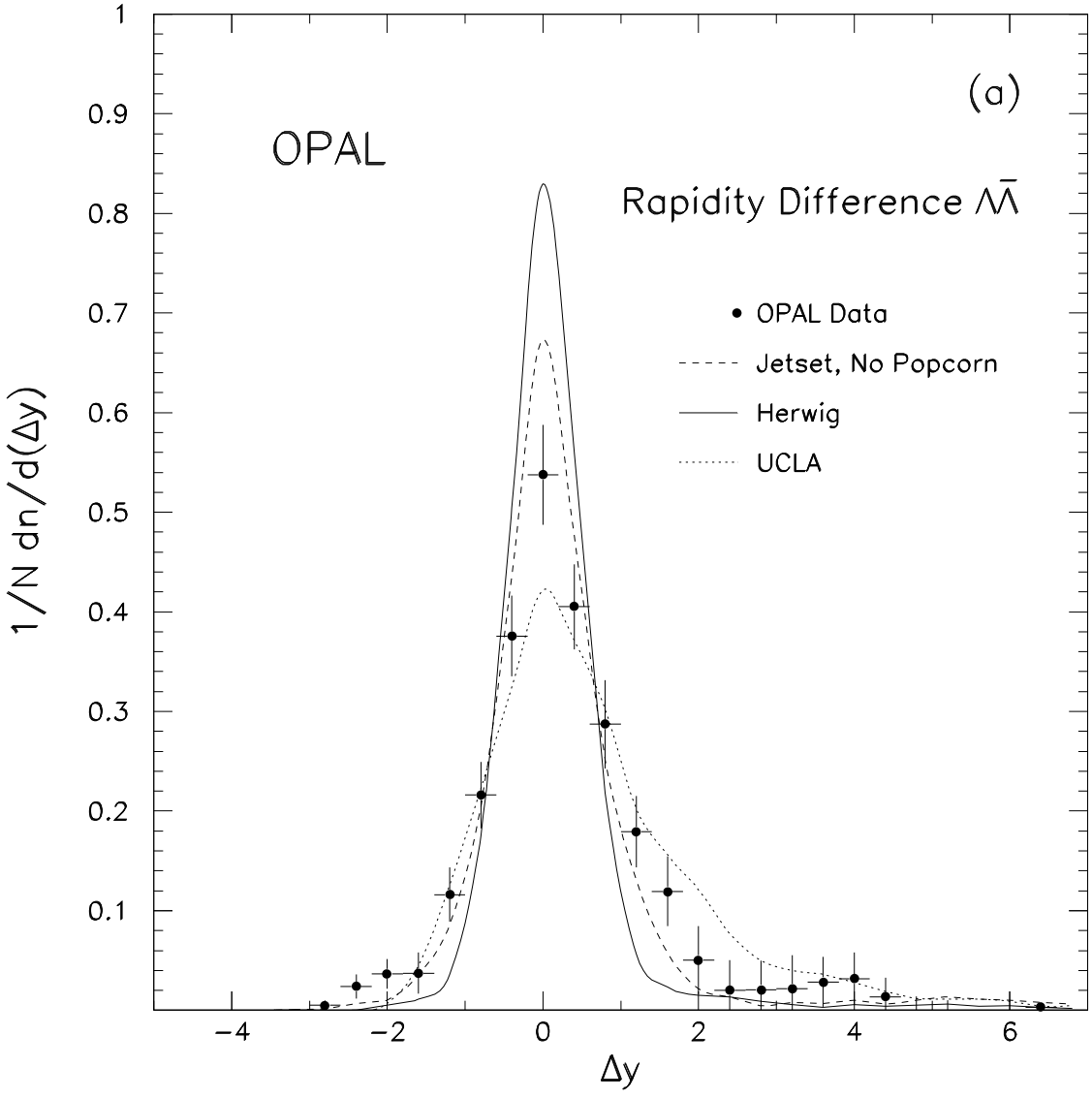
OPAL
(a)
Rapidity Difference $\Lambda\bar{\Lambda}$
OPAL Data
Jetset, No Popcorn
Herwig
UCLA
1/N dn/d(Δy)
Δy
1
0.9
0.8
0.7
0.6
0.5
0.4
0.3
0.2
0.1
−4
−2
0
2
4
6

Figure 6b

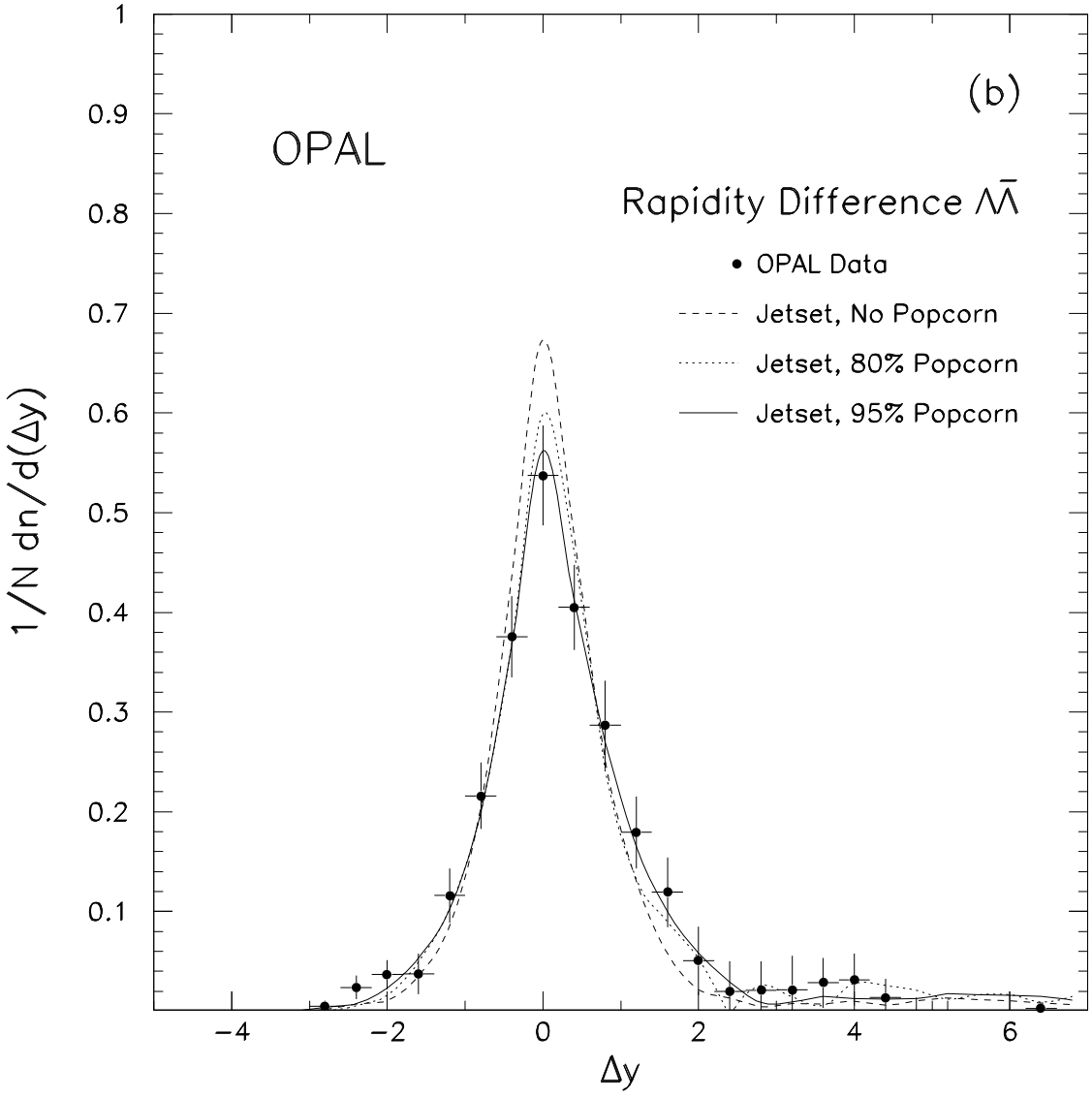
OPAL
(b)
Rapidity Difference $\Lambda\bar{\Lambda}$
OPAL Data
Jetset, No Popcorn
Jetset, 80% Popcorn
Jetset, 95% Popcorn
1/N dn/d(Δy)
Δy
1
0.9
0.8
0.7
0.6
0.5
0.4
0.3
0.2
0.1
−4
−2
0
2
4
6